UNIVERSITÀ DEGLI STUDI DI TORINO

1

Revision 1

3

As-bearing new mineral species from Valletta mine, Maira Valley,

Piedmont, Italy: II. Braccoite, NaMn$^{2+}_5$[Si$_5$AsO$_{17}$(OH)](OH), description and

crystal structure

7

Fernando Cámara[1,2]*, Erica Bittarello[1,2], Marco E. Ciriotti[3], Fabrizio Nestola[4],

Francesco Radica[5] and Marco Marchesini[6]

10

[1]Dipartimento di Scienze della Terra, Università degli Studi di Torino, via Tommaso

Valperga Caluso 35, I-10125 Torino, Italy

[2]CrisDi, Interdepartmental Centre for the Research and Development of Crystallography, via

Pietro Giuria 7, I-10125, Torino, Italy

[3]Associazione Micromineralogica Italiana, via San Pietro 55, I-10073 Devesi-Cirié, Torino,

Italy

[4]Dipartimento di Geoscienze, Università degli Studi di Padova, via Giovanni Gradenigo 6, I-

35131 Padova, Italy

[5]Dipartimento di Scienze Geologiche, Università degli Studi Roma Tre, largo San Leonardo

Murialdo 1, I-00146 Roma, Italy

[6] EEEP house, UNIR, Basing View, Basingstoke, Hampshire, RG21 4YY, United Kingdom

22

*correspondent author's e-mail: fernando.camaraartigas@unito.it

24

25   **ABSTRACT**

26   The new mineral species braccoite, ideally $NaMn^{2+}_5[Si_5AsO_{17}(OH)](OH)$, has been

27   discovered in the Valletta mine dumps, in Maira Valley, Cuneo province, Piedmont, Italy. Its

28   origin is probably related to the reaction between ore minerals and hydrothermal fluids. It

29   occurs as subhedral crystals that occurs in brown-red coloured thin masses, with pale yellow

30   streak and vitreous to resinous luster. Braccoite is associated with tiragalloite, of which new

31   data is provided, as well as gamagarite, hematite, manganberzeliite, palenzonaite, quartz,

32   saneroite,   tokyoite, unidentified Mn oxides, organic compounds, and Mn arsenates and

33   silicates under study.

34   Braccoite is biaxial positive with refractive indices α 1.749(1), β 1.750(1), γ 1.760(1). It

35   is triclinic, space group $P\bar{1}$, with a = 9.7354(4), b = 9.9572(3), c = 9.0657(3) Å, α = 92.691(2)°,

36   β = 117.057(4)°, γ = 105.323(3)°, V = 740.37(4) Å^3 and Z 2. Its calculated density is 3.56

37   g/cm^3. The ten strongest diffraction lines of the observed X-ray powder diffraction pattern are

38   [d in Å, (I), (hkl)]: 3.055 (69)($2\bar{2}1$), 3.042 (43)(102), 3.012 (65)($32\bar{1}$), 2.985 (55)($23\bar{1}$), 2.825

39   (100)($21\bar{3}$), 2.708 (92)(220), 2.627 (43)($23\bar{2}$), 2.381 (58)($4\bar{1}\bar{1}$), 2.226 (25)(214), and 1.680

40   ($43\bar{3}$)(36). Chemical analyses by WDS electron microprobe gave (wt%): Na_2O 4.06, CaO

41   0.05, MnO 41.76, MgO 0.96, Al_2O_3 0.04, CuO 0.02, SiO_2 39.73, As_2O_5 6.87, V_2O_5 1.43, SO_3

42   0.01, and F 0.04. H_2O 2.20 was calculated on the basis of 2OH groups p.f.u. Raman

43   spectroscopy confirmed the presence of $(SiO_4)^{4-}$, $(AsO_4)^{3-}$ and OH groups. The empirical

44   formula calculated on the basis of Σ cations-(Na,K) = 11 p.f.u., in agreement to the results of

45   crystal structure, is $Na_{1.06}(Mn^{2+}_{4.46}Mn^{3+}_{0.32}Mg_{0.19}V^{3+}_{0.01}Al_{0.01}Ca_{0.01})[Si_5(As_{0.48}Si_{0.37}V^{5+}_{0.15})O_{17}$

46    $(OH)](OH_{0.98}F_{0.02})$,   the   simplified   formula   is $Na(Mn,Mg,Al,Ca)_5[Si_5(As,$ V,

47    $Si)O_{17}(OH)](OH,F)$.

48   Single crystal X-ray diffraction allowed us to solve the structure by direct methods and

49   revealed that braccoite is the As-dominant analogue of saneroite. The structure model was

50   refined on the basis of 4389 observed reflections to R_1 3.47 %. Braccoite is named in honor of

51   Dr. Roberto Bracco (b. 1959), a systematic collector with a special interest in manganese

52   minerals. The new mineral was approved by IMA 2013-093.

53

54   **Keywords:** braccoite, saneroite, arseno-silicates, tiragalloite, new mineral species, crystal

55   structure, Raman, Valletta, Piedmont, Italy

56

INTRODUCTION

58   This is the second of a series of new mineral descriptions of As–bearing minerals from

59   Valletta mine (Cámara *et al*. 2014). The sample containing braccoite, the As-analogue of

60   saneroite, was collected by one of the authors (MM) in 2012 in the dumps of Valletta mine,

61   Vallone della Valletta, Canosio municipality, Maira Valley, Cuneo province, Piedmont, Italy

62   (44°23'54" N, 7°5'42" E, 2536 m asl).

63   The name is in honour of Dr. Roberto Bracco (b. 1959), a systematic collector with a

64   special interest in manganese minerals (Barresi *et al.*, 2005; Bracco and Balestra, 2014). He

65   has authored or coauthored several publications on systematic mineralogy, especially devoted

66   to new occurrences in Liguria (Bracco *et al.*, 2006; 2012).

67   A fragment of the holotype material is deposited in the mineralogical collections of the

68   Museo Regionale di Scienze Naturali di Torino, Sezione di Mineralogia, Petrografia e

69   Geologia, Torino, Italy, catalogue number M/15939.

70   Braccoite is intergrown with tiragalloite, which is an infrequent mineral. For this reason

71   we provide additionally chemical and Raman spectrum of tiragalloite [$Mn^{2+}_4As^{5+}Si_3O_{12}(OH)$]

72   from Valletta mine.

73

74   **GEOLOGICAL SETTING AND MINERAL OCCURRENCE**

75   Geological and historical brief information is provided in Cámara *et al*. (2014). The

76   deposit at Valletta mine has never been studied from a genetic point of view and available

77   geological data for the area are of limited detail. Other than the historic texts, there is no

78   mention in the literature of the occurrence of metalliferous mineralization in this locality.

79   Preliminary work carried out during sampling showed that it is a small iron deposit with

80   subordinate manganese, in quartzites with quartz veins that contain a large variety of mineral

81   phases rich in arsenic, vanadium, barium and strontium. The volume of mineralized body is

82   however rather limited in surface.

83   The rock hosting braccoite is compact, granular, dark red verging on black quartzite.

84   Blocks of this material have been dug and piled up in a small landfill where they are mixed

85   with calcareous rocks also from the excavated material.

86   Braccoite is strictly associated with tiragalloite, and with gamagarite, hematite,

87   manganberzeliite, palenzonaite, quartz, saneroite, tokyoite, unidentified Mn oxides, organic

88   compounds, and Mn arsenates and silicates under study. These findings make in terms of

89   mineralogical variety the small dump of the old Valletta mine one of the richest Italian

90   deposits of arsenates and silicoarsenates mineral phases, like those of Val Graveglia (Antofilli

91 *et al.* 1983; Borgo and Palenzona, 1988; Palenzona, 1991, 1996; Marchesini and Pagano,

92 2001). Other As-rich minerals found in the rock samples collected in the dump, although not

93 strictly associated with braccoite are: adelite $CaMg(AsO_4)(OH)$, arseniopleite-caryinite series

94 $(Ca,Na)NaMn^{2+}(Mn^{2+},Mg,Fe^{2+})_2(AsO_4)_3$-$(Na,Pb)(Ca,Na)CaMn^{2+}_2(AsO_4)_3$,

95 bariopharmacosiderite $Ba_{0.5}Al_4(AsO_4)_3(OH)_4 \cdot 4H_2O$, berzeliite $NaCa_2Mg_2(AsO_4)_3$, grandaite

96 $Sr_2Al(AsO_4)_2(OH)$ (IMA2013-059), and tilasite $CaMg(AsO_4)F$; these are found along with

97 aegirine, albite, azurite, baryte, braunite, calcite, diopside, fluorapatite, ganophyllite, gypsum,

98 ilmenite, hollandite, malachite, magnesio-arfvedsonite, magnesio-riebeckite, magnetite,

99 mimetite, muscovite, neotocite, opal, orthoclase, phlogopite, ranciéite, richterite, rutile,

100 rhodonite, talc, tetrahedrite, titanite and some other unknown phases under investigation.

101

102 **MINERALOGICAL CHARACTERIZATION**

103

104 **Appearance and physical properties**

105 Braccoite occurs as subhedral equant crystals, few hundred of micrometers accros,

106 with uneven fracture, grouped in thin masses, a few centimeters in size (Fig. 1), on granular

107 red-brown quartzite with reddish-brownish-black K-feldspar and compact quartz. In rare cases

108 the mineral forms rims around the remnants of protolithic quartz clasts. Individual crystals are

109 brown-red coloured and translucent. Braccoite has a pale yellow streak, a vitreous to resinous

110 luster, and does not fluoresce under SW or LW ultraviolet light. Braccoite is optically biaxial

111 positive, with a $2V_{meas} = 26(2)°$ and $2V_{calc} = 35°$. The measured refractive indices are $\alpha =$

112 1.749(1), $\beta = 1.750(1)$, and $\gamma = 1.760(1)$ (589 nm). Braccoite is weakly pleochroic with X =

113 brownish yellow, Y = dark yellow, Z = yellow. The mineral is brittle and no cleavage and

114 parting are observed. Hardness and density were not measured due to the small crystal size

115 and because it occurs intimately intergrown with tiragalloite. The calculated density obtained

116 from the empirical formula and unit-cell parameters of the single crystal used for the crystal-

117 structure determination is 3.56 g/cm^3.

118

119 **Chemical data**

120 Chemical composition of braccoite was determined using a Cameca SX–50 electron

121 microprobe (WDS mode) at the Department of Geosciences (Università di Padova) on a thin

122 section obtained from the holotype close to the place where the crystal used for the diffraction

123 study was extracted. Major and minor elements were determined at 20 kV accelerating

124 voltage and 20 nA beam current (beam size 2 μm), with 40 to 20 s counting time on both peak

125 and background. X–ray counts were converted to oxide wt% using the PAP correction
126 program supplied by Cameca (Pouchou and Pichoir, 1984; 1985). The crystals studied in the
127 thin section (Fig. 2) were found to be homogeneous. Fe, Sb and Pb were analysed for but
128 were below detection limits. H_2O was calculated on the basis of 2OH groups p.f.u.
129 (Nagashima and Armbruster, 2010a). The average of 5 analyses are given in Table 1a. Low
130 totals are related to the difficulty of preparing good thin sections of polymineralic aggregates,
131 but have been also reported for saneroite samples (Nagashima and Armbruster, 2010a).

132 The empirical formula, calculated on the basis of 19 O a.p.f.u. and considering 2(OH)
133 is, within rounding errors, $Na_{1.06}(Mn^{2+}_{4.46}Mn^{3+}_{0.32}Mg_{0.19}Al_{0.01}Ca_{0.01})_{\Sigma4.99}[(Si_{5.36}As_{0.48}V_{0.15})_{\Sigma5.99}$
134 $O_{17}(OH)](OH_{0.98}F_{0.02})$. Alternatively, the empirical formula, calculated on the basis of Σ
135 cations-(Na,K) = 11, Mn^{2+}/Mn^{3+} ratio calculated in order to obtain [2(OH)-(Na-0.5)] groups
136 p.f.u. $[Mn^{3+}/(total\ Mn) = 0.066]$ and tetrahedral V^{5+} calculated as 6 – (Si + As), and excess V
137 is assigned to the octahedral sites as V^{3+}, following Nagashima and Armbruster (2010a),
138 within rounding errors, is $Na_{1.06}(Mn^{2+}_{4.46}Mn^{3+}_{0.32}Mg_{0.19}V^{3+}_{0.01}Al_{0.01}Ca_{0.01})_{\Sigma=5.00}$
139 $[Si_{5.37}As^{5+}_{0.48}V^{5+}_{0.15}O_{17}(OH)](OH_{0.98}F_{0.01})$. The simplified formula can be written as:
140 $NaMn^{2+}_5[Si_5AsO_{17}(OH)](OH)$, which requires Na_2O 3.78, MnO 43.31, SiO_2 36.68, As_2O_5
141 14.03, and H_2O 2.20, total 100 wt%. The presence of OH was confirmed by micro-Raman
142 spectroscopy. The mean refractive index *n* of braccoite, the calculated density and the
143 empirical formula yielded a Gladstone-Dale compatibility index (Mandarino 1979, 1981) of
144 0.020 rated as excellent. Braccoite is unreactive and insoluble in 2 *M* and 10% HCl, and 65%
145 HNO_3.

146 In Table 1b we show the comparison between the chemical data of tiragalloite
147 $[Mn^{2+}_4As^{5+}Si_3O_{12}(OH)]$ from Valletta mine and tiragalloite from type-locality of Molinello
148 mine (Ne, Val Graveglia, Liguria, Italy) reported by Gramaccioli *et al.* (1980). Considering a
149 stoichiometric H_2O content in order to have one (OH) group per formula unit (p.f.u.), i.e. 1.46
150 wt % of H_2O, and 13 oxygen atoms p.f.u., the formula corresponding to the average of 3
151 analyses is $(Mn^{2+}_{3.92}Mg_{0.06}Na_{0.03})_{\Sigma4.01}(As^{5+}_{0.87}V^{5+}_{0.05}Si^{4+}_{0.09})_{\Sigma1.01}Si_3O_{12}(OH_{0.96}F_{0.04})$.

152

153 **Micro-Raman spectroscopy**
154 The Raman spectrum of braccoite (Fig. 3) was obtained at the Dipartimento di Scienze
155 della Terra (Università di Torino) using a micro/macro Jobin Yvon LabRam HRVIS,
156 equipped with a motorized x-y stage and an Olympus microscope. The backscattered Raman
157 signal was collected with 50× objective and the spectrum was obtained for a non-oriented
158 crystal. The 632.8 nm line of an He-Ne laser was used as excitation; laser power (20 mW)

159   was controlled by means of a series of density filters. The minimum lateral and depth

160   resolution was set to a few μm. The 532 nm line of a Nd laser was also used as excitation;

161   laser power (80 kW) was dosed by means of a series of density filters. An aperture of 200 μm

162   was used to reduce the beam dose. The lateral and depth resolution were about 2 and 5 μm,

163   respectively. The system was calibrated using the 520.6 cm^{-1} Raman band of silicon before

164   each experimental session. Spectra were collected with multiple acquisitions (2 to 6) with

165   single counting times ranging between 20 and 180 s. The spectrum was recorded using the

166   LabSpec 5 program from 200 to 4000 cm^{-1}. Spectra collected with both lasers were

167   equivalent. Spectrum reported in Fig. 3 was collected with the 632.8 nm line of the He-Ne

168   laser.

169   There is a close match between the braccoite spectrum and that of saneroite from type

170   locality of Molinello mine (Graveglia Valley, Liguria, Italy) in the database RRUFF

171   (R060488) (Downs, 2006). All bands observed between 700 and 1000 cm^{-1} are characteristic

172   of the two groups present in braccoite, SiO_4^{4-} and $AsO_3(OH)^{2-}$ (Myneni *et al.*, 1998a,b;

173   Nakamoto, 1986). The spectrum shows intense bands around 829, 907 and 932 (respect to

174   823, 909 and 936 cm^{-1} for saneroite R060488 at RRUFF) and weak peaks at 706 and 748 cm^{-1}

175   (700 and 729 cm^{-1} for saneroite R060488 at RRUFF). The intense peak at 1017 cm^{-1} with a

176   weak shoulder at 1040 cm^{-1} may be assigned to the v_1 symmetric stretching mode of the SiO_4

177   units (Mills *et al.*, 2005) (1011 and 1022 cm^{-1} for saneroite R060488) while the region

178   assigned in the pyroxenes to the stretching modes of the Si-O bonds is present in the braccoite

179   spectrum at 665 cm^{-1} (respect to 660 cm^{-1} for saneroite R060488). Bending modes of O-Si-O

180   are observed at 525 cm^{-1} and 563 cm^{-1} for braccoite, while Raman spectrum of saneroite

181   R060488 shows a single weak band around 523 cm^{-1}. Cation-oxygen vibration modes appear

182   in the low region of the spectrum below 460 cm^{-1}: weak and broad peaks are observed at 226,

183   261, 291, 360, 390 and 451 cm^{-1} (respect to 228, 281, 343, 376, 436 cm^{-1} for saneroite

184   R060488). The Raman spectrum of braccoite shows a broad envelope of overlapping bands

185   centered upon 3361 and 3507 cm^{-1}, which are characteristic of OH stretching modes, in

186   accordance with the presence of hydroxyl groups in the structure (spectrum of saneroite

187   R060488 was collected only for < 1200 cm^{-1}).

188   Tiragalloite is intergrown with braccoite in rocks from Valletta mine. There is no

189   available Raman spectrum for tiragalloite and therefore we collected spectra also for this

190   mineral phase (Fig. 4). The spectrum shows a strong absorption centered at 869 cm^{-1} with

191   three shoulders at 803, 836 and 902 cm^{-1}, two intense peaks at 661 and 647 cm^{-1} and weaker

192   peaks at 960, 975 cm^{-1} and a broad band at ~ 1004 cm^{-1}. As for braccoite and saneroite, the

193   frequency separations between the bands due to the asymmetric and the symmetric stretches

194   of the anionic groups $(SiO_4)^{4-}$ and $(AsO_4)^{3-}$, present tiragalloite vary strongly from one

195   structure to another, and cannot be assigned with conviction (Hawthorne *et al.*, 2013). Bands

196   with frequencies between 250 and 600 cm^{-1} correspond to $(SiO_4)^{4-}$ and $(AsO_4)^{3-}$ vibrations

197   (286, 320, 364, 398, 481, 508 and 549 cm^{-1}), while weak and broad bands lower than 250 cm^{-1}

198   correspond to lattice modes (153, 181 and 218 cm^{-1}). In the region between 1200 and 3000

199   cm^{-1} the spectrum displays a considerable amount of noise (a broad envelope of overlapping

200   bands centered upon 1635, 1702 and 1799 cm^{-1}) and this is a result of the low intensity of the

201   bands. In accordance with the presence of hydroxyl groups in the structure a wide and weak

202   band at ~3100 cm^{-1}. Based on the Libowitzky (1999) correlation, the band at ~ 3100 cm^{-1} can

203   be possibly assigned to the O11–H11…O1 bond present in tiragalloite (O11…O1 = 2.725 Å

204   corresponding to 3257 cm^{-1}, using crystal data provided by Nagashima and Armbruster

205   2010b).

206

207   **X–ray diffraction**

208   The powder X–ray diffraction pattern of braccoite was obtained at CrisDi

209   (Interdepartmental Centre for the Research and Development of Crystallography, Torino, Italy)

210   using an Oxford Gemini R Ultra diffractometer equipped with a CCD area detector, with

211   graphite-monochromatized Mo$K\alpha$ radiation. Indexing of the reflections was based on a

212   calculated powder pattern obtained from the structural model, using the software LAZY

213   PULVERIX (Yvon *et al.*, 1977). Experimental and calculated data are reported in Table 2. The

214   unit–cell parameters refined from the powder data with the software GSAS (Larson and Von

215   Dreele, 1994) are a = 9.756(6), b = 9.961(7), c = 9.087(7) Å, α = 92.23(5)°, β = 117.27(5)°, γ

216   = 105.21(4)°, V = 742.2(9) Å^3.

217   Single-crystal X–ray diffraction data were collected using an Oxford Gemini R Ultra

218   diffractometer equipped with a CCD area detector at CrisDi with graphite-monochromatized

219   Mo$K\alpha$ radiation (λ = 0.71073 Å). A crystal fragment showing sharp optical extinction

220   behaviour was used for collecting intensity data. No crystal twinning was observed. Crystal

221   data and experimental details are reported in Table 3. The intensities of 7946 reflections with

222   $-13 < h < 14$, $-14 < k < 14$, $-13 < l < 13$ were collected to 64.4° 2θ using 1° frame and an

223   integration time of 20 s. Data were integrated and corrected for Lorentz and polarization

224   background effects, using the package CrysAlisPro, Agilent Technologies, Version

225   1.171.36.20 (release 27-06-2012 CrysAlis171.36.24). Data were corrected for empirical

226   absorption using spherical harmonics, implemented in the SCALE3 ABSPACK scaling

227 algorithm. Refinement of the unit-cell parameters was based on 4389 measured reflections
228 with $I > 10\sigma(I)$. At room temperature, the unit-cell parameters are a 9.7354(4), b 9.9572(3), c
229 9.0657(3) Å, α 92.691(2)°, β 117.057(4)°, γ 105.323(3)°, V 740.37(4) Å^3, space group $P\bar{1}$
230 and Z 2. The a:b:c ratio is 0.978:1:0.910. A total of 4911 independent reflections were
231 collected and the structure was solved and refined using the SHELX set of programs
232 (Sheldrick, 2008).

233

234 **DESCRIPTION OF THE STRUCTURE**

235 **Structure model**

236 The crystal structure of braccoite (Figure 5) is topologically identical to that of the
237 hydropyroxenoid saneroite: a single isolated chain of SiO_4 tetrahedra with a five repeat plus
238 an appendix of a sixth tetrahedron where $Si_{1-x}As_x$ substitution occurs ($Si_{1-x}V^{5+}_x$ in saneroite).
239 which repeats laterally by a centre of symmetry forming a layer of tetrahedra parallel (1$\bar{1}$1).
240 Five octahedral sites occupied by Mn (mostly Mn^{2+}, with some Mn^{3+}) form a band which runs
241 parallel to two single chains of tetrahedra attached up and down. Laterally the bands are
242 separated by channels occupied partially by two independent Na sites, one completely
243 occupied and another with partial occupation. The structure of braccoite was therefore refined
244 starting from the atom coordinates of saneroite excluding H sites (Nagashima and Armbruster,
245 2010a). Nomenclature of sites follows therefore those of the aforementioned authors.
246 Scattering curves for neutral and ionized atoms were taken from International Tables for
247 Crystallography (Wilson, 1992). Site-scattering values were refined for the cation sites using
248 two scattering curves contributing proportionally and constrained sum to full occupancy:
249 Mn^{2+} and Mg were used for the sites Mn(1-5); Si^{4+} full occupancy was fixed at the T(1-5)
250 sites, while Si^{4+} and As were used at T(6) site; Na^+ was used for the Na(1) and Na(2) sites,
251 although the occupancy was held fixed at Na(1) and refined at Na(2). After converging, the
252 positions of two H atoms [H(7) and H(19) sites] were located in difference Fourier maps and
253 added to the model; atom coordinates of H sites were refined and isotropic thermal parameters
254 were constrained to be 1.2 times the isotropic equivalent of the oxygen atom of the hydroxyl
255 group assuming a riding motion model, while a soft constraint of 0.98 Å (Franks, 1973) was
256 applied to the H(19)–O(19) distance. Structure refinement converged to $R_1 = 0.0347$ for 4389
257 reflections with $F_o > 4\sigma(F_o)$ and 0.0413 for all 4911 data. Tables 4, 5 and 6 report atomic
258 coordinates, the displacement parameters and selected bond distances and angles respectively
259 for braccoite. Bond valence calculations using the parameters of Brown (1981) are reported in
260 Table 7. (CIF[1] and structure factor list files are available on deposit).

261

Site occupancies

Cation sites

There are 13 cation sites in the braccoite structure: 6 sites are 4-coordinated, 5 sites are 6-coordinated, and 2 are 8-coordinated. One out of the six 4-coordinated sites, the $T(6)$ site, has a higher mean atomic number [24.17(6) electrons per site (e.p.s.) versus 14 e.p.s. for the other 5 sites, Table 4], and <T-O> is larger than that the other 5 sites (1.675 Å vs. a mean of 1.624 Å for the other 5 sites, Table 6). Chemical analyses report the presence of both V^{5+} and As^{5+} that can order in a site with tetrahedral coordination. The refined site scattering is > 23 e.p.s. and therefore implies dominance of As in presence of sufficient amount of Si. The latter is confirmed by EMP analyses (Table 1a). In presence of concomitant Si-V-As solid solution in a cation site with tetrahedral coordination, the size of the tetrahedron is not sufficient to provide the actual dominance of As^{5+} versus V^{5+} because they have very similar ionic radii (0.335 and 0.355 Å, respectively, Shannon 1976). While distances observed in the studied crystal (Table 6) are compatible with a Si–V substitution (values of 1.68-169 Å are usually found for saneroite, Nagashima and Armbruster, 2010a, and ca. 1.70 Å for medaite, Nagashima and Armbruster, 2010b), It is worth noting that besides the chemical strain due to a three component solid solution, the $T(6)$ is not the most distorted 4-coordinated site in the structure: the $T(5)$ shows the highest angle variance [σ^2 41.72, computed according to Robinson *et al*. 1971, Table 6] as similarly observed in saneroite (σ^2 = 40.00, Basso and Della Giusta, 1980).

Regarding the 5 sites 6-coordinated, all are Mn^{2+} dominant. However, site $Mn(3)$ is significantly smaller (2.183 Å versus 2.20-2.25 Å, Table 6). This can be interpreted as ordering of a lighter and smaller Mg cation, which is present in the chemical analyses. Yet ordering all the Mg at the $Mn(3)$ site would require a site scattering value lighter than that observed. On the other hand, a small quantity of Mn^{3+} has been inferred in the chemical formula (see Chemical data section) in order to achieve charge balance assuming full occupancy of H at the $H(7)$ and $H(19)$ sites. In addition, Nagashima and Armbruster (2010a) confirmed the presence of a limited quantity of Mn^{3+} in saneroite form Molinello (Val Graveglia, Italy) by using the ratio of the X-ray intensities of the Mn$L\beta$ and Mn$L\alpha$ lines after the method of Albee and Chodos (1970) and Kimura and Akasaka (1999). Therefore, we assumed also for braccoite a limited amount of Mn^{3+} (0.066 Mn^{3+}/Mn_{total}). Incidentally, other Mn^{3+} phases have been found at the Valletta mine (es. grandaite, Cámara *et al*., 2014) and all the iron–bearing phases have just Fe^{3+}. Because there is not a high bond valence contribution

295 to the $Mn(3)$ site (Table 7) it is probable that Mn^{3+} distributes also in the other two smaller

296 sites, $Mn(2)$ and $Mn(4)$. In the structure of braccoite there is also one octahedron that is

297 slightly larger than the others, the $Mn(1)$ site. Apparently, it should host the very small

298 amount of Ca in the analyses, although that amount is not enough to justify the observed size

299 enlargement. However, Ca could also distribute at the $Na(1)$ or $Na(2)$ sites. The $Mn(1)$ site is

300 also the more distorted (σ^2 = 170.51, compared to values ranging between 55.18 and 86.77,

301 Table 6). This is possibly due to the fact that the oxygen at O(16) acts as bond donor to the

302 proton at $H(19)$ and that it is the only octahedron that shares an edge with a tetrahedron, the

303 $T(5)$ site, which is also the most distorted tetrahedron. The O(5)-O(14) edge involves two

304 anion sites with among the highest and the lowest bond valence contribution, respectively

305 (Table 7) and is also the shortest. Hence there is a possible charge-shielding mechanism

306 operated by the electronic clouds of both oxygen atoms.

307   The 8-coordinated sites host Na atoms. The $Na(1)$ site has full occupancy and bond

308 distances compatible with 1 a.p.f.u. of Na (Table 8), while the $Na(2)$ site shows a refined site

309 scattering which indicates approx. half occupancy of Na (Table 4). This site shares four edges

310 with four Si tetrahedra and two edges with two Mn octahedra [$Mn(2)$ and $Mn(5)$]. This is

311 probably impeding the full occupancy of this site and produces a rather distorted bonding

312 environment.

313   Taking into consideration the observed site scattering values and those obtained from

314 EMP analyses, the agreement for all cations sites is within 2% relative error, with slightly

315 lighter values from diffraction data than obtained from chemical analyses (230.8 electrons per

316 formula unit, e.p.f.u., versus 233.9 e.p.f.u., respectively). Site-distribution according to the

317 structure refinement (site scattering and bond distances) and electron microprobe data results

318 give full occupancy of Si at the $T(1\text{-}5)$ sites, $T6$ ($As^{5+}_{0.48}Si_{0.37}V^{5+}_{0.15}$), $Mn1$

319 ($Mn^{2+}_{0.98}Mg_{0.01}Ca_{0.01}$), $Mn2$ ($Mn^{2+}_{0.87}Mn^{3+}_{0.07}Mg_{0.06}$), $Mn3$

320 ($Mn^{2+}_{0.66}Mn^{3+}_{0.22}V^{3+}_{0.01}Al_{0.01}Mg_{0.10}$), $Mn4$ ($Mn^{2+}_{0.96}Mn^{3+}_{0.03}Mg_{0.01}$), $Mn5$ ($Mn^{2+}_{0.99}Mg_{0.01}$),

321 $Na1$ ($Na_{1.00}$), $Na2$ ($Na_{0.56}$), with an overall positive charge of 36.53. Table 8 reports the

322 agreement between observed values and those calculated from chemical composition after site

323 assignment.

324

325   *Anion sites*

326   There are 19 anion sites in the structure of braccoite, 10 are 3-coordinated and the rest

327 are 4-coordinated (Table 7). There are three anion sites with a bond valence incidence

328 significantly higher than 2 v.u.: O(4), O(5) and O(6). The same atoms show also high bond

329   valence incidence for saneroite (Basso and Della Giusta, 1980; Nagashima and Armbruster

330   2010a), in particular O(4), which is 3-coordinated; at the O(4) site, the contribution from $T(3)$

331   and $T(4)$ is already 2.011 v.u. and therefore the contribution from the $Na(2)$ site (0.134 v.u.,

332   Table 7) oversaturates this anion site. This is in fact a strong another restriction for a full

333   occupancy of the $Na(2)$ site (see above).

334   Two anion sites are actually 3-coordinated [O(11) and O(16)] but act as donor of two

335   respective hydrogen bonds at O(7) and O(19). Chemical analyses show a very limited amount

336   of fluorine. While it is not possible to assess in which site the fluorine orders, it is highly

337   probable that it orders at the O(19) site: this site receives a bond valence contribution of 1.091

338   v.u. (Table 7) and therefore hosts an (OH) group, which belongs to three octahedra of two

339    $Mn(3)$ and one $Mn(2)$ site. The Raman spectrum at Figure 3 shows a broad envelope of

340   overlapping bands centered upon 3361 and 3507 cm^{-1}, which are reflecting the two essential

341   next neighbor configurations: $Mn^{2+}Mn^{2+}Mn^{2+}$ and $Mn^{3+}Mn^{3+}Mn^{2+}$, while other configurations

342   are also possible, i.e. $MgMgMn^{2+}$, $Mn^{3+}Mn^{3+}Mn^{3+}$ or even MgMgMg, yielding in the overall

343   a broad band. Hydrogen bonding is also present at the O(7) anion site. However, in this case,

344   a short distance with another oxygen atom at the O(11) anion site (2.48 Å) along with a

345   similar bond valence contribution, of 1.531 for O(7) and 1.524 v.u. for O(11), is probably

346   responsible for a very strong hydrogen bond (see later).

347

348   **Hydrogen bonding**

349   Strong hydrogen bonding is present in the braccoite structure as it was observed in

350   saneroite. A close inspection of Table 7 shows that there are four oxygen sites with bond

351   valence incidence < 1.8 v.u: O(7), O(11), O(16) and O(19). There is one very short acceptor-

352   donor distance corresponding to a very strong hydrogen bond [O(7)…O(11) = 2.48 Å, Table

353   6], and another longer distance corresponding to a medium strength hydrogen bond

354   (O(19)…O(16)   =   2.855   Å,   Table   6).   Using   the   relation $v(\text{cm}^{-1})$ =

355    $3592 - 304 \times 10^{9} \cdot \exp(-d(\text{O}…\text{O})/0.1321)$ (Libowitzky, 1999), we should expect bands at 1456

356   and 3467 cm^{-1}. While frequencies at ca. 3500 cm^{-1} are observed in the Raman spectrum of

357   braccoite (Fig. 3) the expected band around 1400 cm^{-1} is not visible in the spectrum. The

358   positions of two hydrogen atoms were observed in the Fourier-difference maps at

359   convergence and were added to the model. In particular, the position observed for the $H(7)$

360   atom shows a bond with oxygen at the O(7) anion site with a short $H(7)…O(11)$ distance of

361   1.62(4) Å. The position of the corresponding hydrogen atom in saneroite was not detected by

362   Basso   and   Della   Giusta   (1980)   but   was   found   with   very   similar   atom   coordinates   by

363   Nagashima and Armbruster (2010a) ($x = 0.937(5)$ $y = 0.493(4)$ $z = 0.820(5)$ for braccoite and

364    $x = 0.940(3)$ $y = 0.506(3)$ $z = 0.815(4)$ for saneroite specimen 1 of Nagashima and

365   Armbruster, 2010a, Table 3), and in fact a band at ca. 1400 cm^{-1} was observed in the FT-IR

366   spectrum collected on saneroite from Molinello by Brugger *et al*. (2006). The fact that both

367   O(7) and O(11) show an equivalent bond valence contribution (Table 7), suggests a plausible

368   disordered environment for this proton. Such a situation, with a disordered position for H, has

369   been already observed in another related pyroxenoid structure, serandite

370   (NaMn$_2$[Si$_3$O$_8$(OH)]), which shows a O…O distance of 2.464–2.468 Å (Jacobsen *et al*., 2000)

371   and for which the IR O–H stretching mode was found at 1386 cm^{-1} (Hammer *et al*., 1998).

372   Another topologically related structure is scheuchzerite (NaMn$^{2+}_9$[Si$_9$V^{5+}O$_{28}$(OH)](OH)$_3$;

373   Brugger *et al*., 2006), which has also a very strong hydrogen bond among O(26) and O(29)

374   anion sites, distant by 2.35 Å (Brugger *et al*., 2006). In this case a band is observed at 1466

375   cm^{-1} in the FTIR spectrum, which can correspond to the strong hydrogen bond. It should be

376   also taken into account that the *H*(7) site is at a distance of 2.09(5) Å of the *Na*(2) site, which

377   is not far of the Na-H distance in NaH (1.913 Å; Chen *et al*., 2005) and this surely stresses the

378   bonding environment of the proton at ca. half of the *H*(7) sites.

379

380   **RELATED MINERALS**

381   Braccoite, NaMn$^{2+}_5$[Si$_5$AsO$_{17}$(OH)](OH), is the As–dominant analogue of saneroite,

382   NaMn$^{2+}_5$[Si$_5$V^{5+}O$_{17}$(OH)](OH) (Basso and Della Giusta, 1980; Lucchetti *et al*., 1981;

383   Nagashima and Armbruster, 2010a). For the dominant cation in *T*6 site Nagashima and

384   Armbruster (2010) proposed to add a suffix, i.e. "saneroite-(V)", "saneroite-(Si)" and

385   "saneroite-(As)". In the recent IMA guidelines, Hatert *et al*. (2013) allow the use of any

386   another name confirming that "mineral names are chosen by the authors of new mineral

387   species, according to functional guidelines established by the Nickel & Grice (1998)" . A new

388   name was chosen to avoid suffixing saneroite so as to preserve *in toto* this "well-established

389   name" and also to meet with the preferences of the collectors community.

390   Braccoite has also structural similarity with scheuchzerite,

391   NaMn$^{2+}_9$[Si$_9$V^{5+}O$_{28}$(OH)](OH)$_3$ (Brugger *et al*., 2006; Palenzona *et al*., 2006; Roth, 2007):

392   while saneroite/braccoite have a silicate single-chain with five tetrahedra in the repeating unit

393   – with an additional tetrahedron branching sideways (Fig. 5) – scheuchzerite has a chain that

394   consists of the branched saneroite chain with additional attached silicate tetrahedra,

395   configuring "loops" (Brugger *et al*., 2006). These "loops" are also present in a new Na-Mn

396   borosilicate, steedite NaMn$^{2+}_2$[Si$_3$BO$_9$(OH)](OH) (IMA2013-052), which crystal structure

397 closely resembles those of the sérandite-pectolite pyroxenoids and it is also broadly similar to
398 the crystal structure of scheuchzerite (Haring and McDonald, 2014).

399   Braccoite is the first As member of the saneroite family and in Table 9 we have
400 reported a comparison of the properties of the members. In the Strunz System (Strunz and
401 Nickel, 2001) braccoite fits in subdivision 9.D.K, inosilicates with 5-periodic single chains.
402 Its equivalent synthetic compound is not known.

403

411

412 **REFERENCES**
413 Albee, A. and Chodos, A.A. (1970) Semiquantitative electron microprobe determination of
414   Fe^{2+}/Fe^{3+} and Mn^{2+}/Mn^{3+} in oxides and silicates and its application to petrologic
415   problems. *American Mineralogist*, **55**, 491−501.
416 Albrecht, J. (1990) An As-rich manganiferous mineral assemblage from the Ködnitz Valley
417   (Eastern Alps, Austria): geology, mineralogy, genetic considerations, and implications for
418   metamorphic Mn deposits. *Neues Jahrbuch für Mineralogie, Monatshefte*, 363−375.
419 Antofilli, M., Borgo, E., and Palenzona, A. (1983) *I nostri minerali. Geologia e mineralogia*
420   *in Liguria*, 296 p. SAGEP Editrice, Genova (in Italian). Barresi, A.A., Kolitsch, U.,
421   Ciriotti, M.E., Ambrino, P., Bracco, R., and Bonacina, E. (2005) La miniera di
422   manganese di Varenche (Aosta, Italia nord-occidentale): ardennite, arseniopleite,
423   manganberzeliite, pirofanite, sarkinite, thortveitite, nuovo As−Sc−analogo della
424   metavariscite e altre specie. *Micro*, **3**, 81−122 (in Italian).
425 Basso, R., and Della Giusta, A. (1980) The crystal structure of a new manganese silicate.
426   *Neues Jahrbuch für Mineralogie, Abhandlungen*, **138**, 333−342.
427 Bracco, R. and Balestra, C. (2014) La miniera di Monte Nero, Rocchetta Vara, La Spezia,
428   Liguria: minerali classici e novità. *Micro*, **12**, 2−28 (in Italian).

429 Bracco, R., Balestra, C., Castellaro, F., Mills, S.J., Ma, C., Callegari, A.M., Boiocchi, M.,

430   Bersani, D., Cadoni, M., and Ciriotti, M.E. (2012) Nuovi minerali di Terre Rare da Costa

431   Balzi Rossi, Magliolo (SV), Liguria. *Micro*, **10**, 66−77 (in Italian).

432 Bracco, R., Callegari, A., Boiocchi, M., Balestra, C., Armellino, G., and Ciriotti, M.E. (2006)

433   Costa Balzi Rossi (Magliolo, Val Maremola, Savona, Liguria): una nuova località per

434   minerali di Terre Rare e scandio. *Micro*, **4**, 161−178 (in Italian).

435 Borgo, E. and Palenzona, A. (1988) *I nostri minerali. Geologia e mineralogia in Liguria.*

436   *Aggiornamento* 1988, 48 p. SAGEP Editrice, Genova (in Italian).

437 Brown, I.D. (1981) The bond-valence method: an empirical approach to chemical structure

438   and bonding. Pp. 1–30. *Structure and Bonding in Crystals* II, (M. O'Keeffe and A.

439   Navrotsky, editors), Academic Press, New York.

440 Brugger, J., Krivovichev, S., Meisser, N., Ansermet, S., and Armbruster, T. (2006)

441   Scheuchzerite, $Na(Mn,Mg)_9[VSi_9O_{28}(OH)](OH)_3$, a new single-chain silicate. *American*

442   *Mineralogist*, **91**, 937−943.

443 Cámara, F., Ciriotti, M.E., Bittarello, E., Nestola, F., Massimi, F., Radica, F., Costa, E.,

444   Benna, P., and Piccoli, G.C. (2014) As−bearing new mineral species from Valletta mine,

445   Maira Valley, Piedmont, Italy: I. Grandaite, $Sr_2Al(AsO_4)_2(OH)$, description and crystal

446   structure. *Mineralogical Magazine*, (in press).

447 Chen Y.L., Huang, C.H. and Hu, W.P. (2005) Theoretical study of the small clusters of LiH,

448   NaH, BeH_2, and MgH_2. *The Journal of Physical Chemistry* A, **109**, 9627−9636.

449 Downs, R.T. (2006) The RRUFF Project: an integrated study of the chemistry,

450   crystallography, Raman and infrared spectroscopy of minerals. Program and Abstracts of

451   the 19th General Meeting of the International Mineralogical Association in Kobe, Japan.

452   O03-13

453 Franks, F., ed. (1973): Water: a comprehensive treatise, Vol. 2. Plenum, New York, 684 p.

454 Gramaccioli C. M., Griffin W.L., Mottana A. (1980) Tiragalloite, $Mn_4[AsSi_3O_{12}(OH)]$, a new

455   mineral and the first example of arsenatotrisilicate. *American Mineralogist*, **65**, 947−952.

456 Hammer, V.M.F., Libowitzky, E., Rossman, G.R. (1998) Single crystal IR spectroscopy of

457   very strong hydrogen bonds in pectolite, $NaCa_2[Si_3O_8(OH)]$, and serandite,

458    $NaMn_2[Si_3O_8(OH)]$. *American Mineralogist*, **83**, 569–576.

459 Haring, M.M.M., McDonald A.M. (2014) Steedeite, $NaMn_2[Si_3BO_9](OH)_2$: characterization,

460   crystal-structure determination, and origin. *Canadian Mineralogist*, **52**, 47-60.

461 Hatert, F., Mills, S.J., Pasero, M., Williams, P.A. (2013) CNMNC guidelines for the use of

462   suffixes and prefixes in mineral nomenclature, and for the preservation of historical

463   names. *European Journal of Mineralogy*, **25**, 113–115.

464 Hawthorne F.C., Abdu Y.A., Ball N.A, Pinch W.W. (2013) Carlfrancisite:

465      $Mn^{2+}_3(Mn^{2+},Mg,Fe^{3+},Al)_{42}(As^{3+}O_3)_2(As^{5+}O_4)_4[(Si,As^{5+})O_4]_6[(As^{5+},Si)O_4]_2(OH)_{42}$, a new

466   arseno-silicate mineral from the Kombat mine, Otavi Valley, Namibia. *American*

467   *Mineralogist*, **98**, 1693−1696.

468 Jacobsen, S.D., Smyth, J.R., Swope, R.J., Sheldon, R.I. (2000) Two proton positions in the

469   very strong hydrogen bond of serandite, $NaMn_2[Si_3O_8(OH)]$. *American Mineralogist*, **85**,

470   745–752.

471 Kimura, Y. and Akasaka, M. (1999) Estimation of Fe^{2+}/Fe^{3+} and Mn^{2+}/Mn^{3+} ratios by electron

472   probe micro analyzer. *Journal of the Mineralogical Society of Japan*, **28**, 159–166 (in

473   Japanese with English abstract).

474 Larson, A.C., and Von Dreele, R.B. (1994) General Structure Analysis System (GSAS). Los

475   Alamos National Laboratory Report LAUR, 86−748.

476 Libowitzky, E. (1999) Correlation of OH stretching frequencies and O–H…O hydrogen bond

477   lengths in minerals. *Monatshefte für Chemie*, **130**, 1047–1059.

478 Lucchetti, G., Penco, A.M., and Rinaldi, R. (1981) Saneroite, a new natural hydrated Mn-

479   silicate. *Neues Jahrbuch für Mineralogie, Monatshefte*, 161−168.Mandarino, J.A. (1979)

480   The Gladstone-Dale relationship. Part III. Some general applications. *The Canadian*

481   *Mineralogist*, **17**, 71−76.

482 Mandarino, J.A. (1981) The Gladstone-Dale relationship. Part IV. The compatibility concept

483   and its application. *The Canadian Mineralogist*, **19**, 441–450.

484 Marchesini, M. and Pagano, R. (2001) The Val Graveglia Manganese District, Liguria, Italy.

485   *Mineralogical Record*, **32**, 349−379.

486 Mills, S.J., Frost, R.L., Kloprogge, J.T., and Weier, M.L. (2005) Raman spectroscopy of the

487   mineral rhodonite. *Spectrochimica Acta*, **62**, 171−175.

488 Momma, K. and Izumi, F. (2011) "VESTA 3 for three-dimensional visualization of crystal,

489   volumetric and morphology data. Journal of Applied Crystallography, **44**, 1272−1276.

490 Myneni, S.C.B., Traina, S.J., Waychunas, G.A., and Logan, T.J. (1998a) Experimental and

491   theoretical vibrational spectroscopic evaluation of arsenate coordination in aqueous

492   solutions and solids. *Geochimica et Cosmochimica Acta*, **62**, 3285−3300.

493 Myneni, S.C.B., Traina, S.J., Waychunas, G.A., and Logan, T.J. (1998b) Vibrational

494   spectroscopy of functional group chemistry and arsenate coordination in ettringite.

495   *Geochimica et Cosmochimica Acta*, **62**, 3499−3514.

496 Nakamoto, K. (1986) Infrared and Raman Spectra of Inorganic and Coordination Compounds,

497   419 pp. Wiley, New York.

498 Nagashima, M., and Armbruster, T. (2010a) Saneroite: chemical and structural variations of

499   manganese pyroxenoids with hydrogen bonding in the silicate chain. *European Journal*

500   *of Mineralogy*, **22**, 393−402.

501 Nagashima, M., and Armbruster, T. (2010b) Ardennite, tiragalloite and medaite: structural

502   control of $(As^{5+},V^{5+},Si^{4+})O_4$ tetrahedra in silicates. *Mineralogical Magazine*, **74**, 55−71.

503 Palenzona, A. (1991) *I nostri minerali. Geologia e mineralogia in Liguria. Aggiornamento*

504   1990, p. 48. Amici Mineralogisti Fiorentini, Associazione Piemontese Mineralogia

505   Paleontologia & Mostra Torinese Minerali, Centro Mineralogico Varesino, Gruppo

506   Mineralogico "A. Negro" Coop Liguria (GE), Gruppo Mineralogico Lombardo, Gruppo

507   Mineralogico Paleontologico "3M" Ferraia (Savona), (in Italian).

508 Palenzona, A. (1996) *I nostri minerali. Geologia e mineralogia in Liguria, Aggiornamento*

509   1995. Rivista Mineralogica Italiana, 2, 149−172 (in Italian).

510 Palenzona, A., Martinelli, A., Bracco, R., and Balestra, C. (2006) IMA 2004-044

511   (scheuchzerite) alla miniera di Gambatesa. *Prie*, **2**, 11−12 (in Italian)

512 Pouchou, J.L., and Pichoir, F. (1984) A new model for quantitative analysis: Part I.

513   Application to the analysis of homogeneous samples. *La Recherche Aerospatiale*, **3**,

514   13−38.

515 Pouchou, J.L., and Pichoir, F. (1985) `PAP' $\varphi(\rho Z)$ procedure for improved quantitative

516   microanalysis. In J.T. Armstrong, Ed., *Microbeam Analysis*, p. 104−106. San Francisco

517   Press, San Francisco, California.

518 Robinson, K., Gibbs, G.V., and Ribbe, P.H. (1971) Quadratic elongation: a quantitative

519   measure of distortion in coordination polyhedra. *Science*, **172**, 567−570.

520 Roth, P. (2007) Scheuchzerite. In Minerals First Discovered in Switzerland and Minerals

521   Named after Swiss Individuals. Kristallografik Verlag, Achberg, p.130−131.

522 Shannon, R.D. (1976) Revised effective ionic radii and systematic studies of interatomie

523   distances in halides and chaleogenides. *Acta Crystalographica*, **32**, 751−767.

524 Strunz, H., and Nickel, E.H. (2001) Strunz Mineralogical Tables. Chemical Structural Mineral

525   Classification System. 9th Ed., 870 pp. Schweizerbart, Stuttgart.

526 Sheldrick, G.M. (2008) A short history of SHELX. *Acta Crystallographica*, **A64**, 112–122.

527   Wilson, A.J.C. (editor) (1992) *International Tables for Crystallography. Volume C:*
528   *Mathematical, physical and chemical tables*. Kluwer Academic Publishers, Dordrecht,
529   The Netherlands.
530   Yvon, K., Jeitschko, W., and Parthé, E. (1977) LAZY PULVERIX, a computer program, for
531   calculating X-ray and neutron diffraction powder patterns. *Journal of Applied*
532   *Crystallography*, **10**, 73−74.

TABLES

Table 1a.

	Wt.%	Range	SD	Probe standard (line)
Na_2O	4.06	3.72-4.22	0.20	albite Amelia (Na$K\alpha$)
CaO	0.05	0.03-0.06	0.01	diopside (Ca$K\alpha$)
MgO	0.96	0.90-1.01	0.05	synthetic periclase (Mg$K\alpha$)
MnO	41.76	40.94-42.46	0.41	MnTiO$_3$ (Mn$K\alpha$)
Mn_2O_3***	3.07	2.55-3.87	0.53	
Al_2O_3	0.04	0.01-0.12	0.04	corundum (Al$K\alpha$)
CuO	0.02	0.01-0.04	0.01	metallic Cu (Cu$K\alpha$)
SiO_2	39.73	38.70-40.21	0.59	diopside (Si$K\alpha$)
As_2O_5	6.87	6.10-7.79	0.61	synthetic AsGa (As$L\alpha$)
V_2O_5**	1.43	1.35-1.61	0.11	vanadinite (V$K\alpha$)
SO_3	0.01	0.01-0.02	0.01	sphalerite (S$K\alpha$)
F	0.04	0.00-0.19	0.00	fluorite (F$K\alpha$)
H_2O*	2.20	2.12-2.24		
O = F	-0.02	0.08-0.00		
Total	97.44	96.85-98.26		

Notes: * H_2O calculated in order to have 2(OH) p.f.u.; **total V is reported as V_2O_5 but tetrahedral V^{5+} is calculated as $6 - (Si + As)$, and excess V is assigned to the octahedral sites as V^{3+}, following Nagashima and Ambruster (2010a); ***Mn^{2+}/Mn^{3+} ratio calculated (Mn^{3+}/total Mn = 0.066) in order to obtain 2(OH) groups p.f.u. and V distributed as reported.

Table 1a. Chemical data for braccoite (5 analytical points)

Table 1b.

Wt %	Valletta mine, Italy (1)	Molinello mine, Italy (2)	Ködnitz Valley, Austria (3)
As_2O_5	16.91	16.07	18.35
V_2O_5	0.59	1.67	
Sb_2O_5	0.01		
SiO_2	31.45	32.38	31.91
TiO_2			0.02
Al_2O_3			0.02
FeO	-	0.17	0.56
MnO	46.88	48.34	46.02
CaO	0.27	0.75	0.75
MgO	0.39	-	0.00
PbO	0.04		
SO_3	0.03	-	
Na_2O	0.01		0.03
F	0.11		
O=F	0.05		
Total	96.59	99.38	97.66

(1) this work (average of 3 analytical points); (2) Gramaccioli et al. (1980); (3) Albrecht (1990)

Table 1b. Comparison of chemical data available for tiragalloite from other localities.

Table 2.

h	k	l	d_{obs}(Å)	d_{calc} (Å)	Int. (obs)	Int. (calc)	h	k	l	d_{obs}(Å)	d_{calc} (Å)	Int. (obs)	Int. (calc)
1	$\bar{1}$	1	4.785	4.798	8	7.8	2	$\bar{2}$	2	2.393	2.399	9	2.3
0	2	0	4.723	4.710	8	10.2	0	4	$\bar{1}$	2.388	2.388	22	6.1
2	$\bar{2}$	$\bar{1}$	3.850	3.842	7	6.1	**4**	**$\bar{1}$**	**$\bar{1}$**	**2.381**	**2.378**	**58**	**18.7**
2	$\bar{1}$	$\bar{2}$	3.836	3.820	21	7.6	0	4	0	2.361	2.355	11	2.9
1	1	1	3.785	3.767	7	6.5	2	2	1	2.283	2.271	12	14.8
0	2	1	3.763	3.741	16	14.7	**2**	**1**	**4**	**2.226**	**2.224**	**25**	**13.6**
2	$\bar{2}$	0	3.741	3.748	9	7.3	0	4	$\bar{2}$	2.218	2.223	20	11.3
2	1	$\bar{2}$	3.522	3.516	8	1.6	3	4	$\bar{1}$	2.204	2.202	21	24.8
0	1	2	3.438	3.420	10	1.1	1	0	4	2.186	2.181	6	4.1
1	2	$\bar{2}$	3.337	3.341	19	10.0	2	$\bar{3}$	$\bar{3}$	2.185	2.172	8	4.5
1	$\bar{3}$	0	3.310	3.308	8	8.1	3	4	$\bar{2}$	2.091	2.084	9	5.5
1	$\bar{2}$	$\bar{2}$	3.212	3.192	9	3.5	1	2	4	2.082	2.084	10	14.1
1	$\bar{1}$	2	3.143	3.147	19	27.2	3	1	1	2.067	2.060	12	13.9
1	$\bar{3}$	$\bar{1}$	3.055	3.042	6	2.4	5	$\bar{1}$	4	1.779	1.773	7	6.5
2	**$\bar{2}$**	**1**	**3.055**	**3.064**	**69**	**55.4**	3	1	2	1.738	1.732	7	7.0
1	$\bar{3}$	1	3.054	3.063	17	18.2	1	2	$\bar{5}$	1.693	1.694	9	5.5
1	**0**	**2**	**3.042**	**3.037**	**43**	**15.2**	4	$\bar{5}$	0	1.680	1.683	24	15.3
3	**$\bar{2}$**	**$\bar{1}$**	**3.012**	**3.010**	**65**	**26.9**	**4**	**3**	**-3**	**1.680**	**1.676**	**36**	**25.9**
2	$\bar{3}$	0	2.998	3.002	6	4.7	4	$\bar{2}$	$\bar{5}$	1.655	1.648	14	14.7
2	**$\bar{3}$**	**$\bar{1}$**	**2.985**	**2.979**	**55**	**31.5**	3	$\bar{3}$	3	1.595	1.599	7	5.7
1	0	$\bar{3}$	2.974	2.967	8	4.7	0	5	2	1.595	1.586	13	13.7
2	**1**	**$\bar{3}$**	**2.825**	**2.822**	**100**	**100.0**	4	0	2	1.545	1.542	7	6.1
2	**2**	**0**	**2.708**	**2.696**	**92**	**72.7**	0	3	$\bar{5}$	1.537	1.540	6	5.1
1	1	2	2.699	2.687	6	10.0	5	$\bar{3}$	$\bar{5}$	1.495	1.488	9	7.8
1	3	0	2.673	2.661	20	10.8	3	$\bar{1}$	-6	1.485	1.480	7	2.9
3	0	$\bar{3}$	2.655	2.647	12	17.8	6	0	$\bar{5}$	1.440	1.436	6	2.4
2	**$\bar{3}$**	**$\bar{2}$**	**2.627**	**2.614**	**43**	**29.4**	1	0	5	1.434	1.431	15	13.2
0	1	3	2.433	2.422	15	18.1	6	$\bar{3}$	0	1.434	1.434	15	12.7

Notes: *Only reflections with $I_{rel} > 6\sigma(I_{rel})$ are listed; differences in observed and calculated intensities are related to preferred orientation

Table 2. Observed and calculated X-ray powder diffraction data for braccoite. The ten strongest reflections are reported in bold *

Table 3.

Crystal system	Triclinic
Space group	$P\bar{1}$
Unit–cell dimensions	
a (Å)	9.7354(4)
b (Å)	9.9572(3)
c (Å)	9.0657(3)
α (°)	92.691(2)
β (°)	117.057(4)
γ (°)	105.323(3)
V (Å^3)	740.37(4)
Z	2
μ (mm^{-1})	5.62
$F(000)$	758.78
D_{calc} (g cm^{-3})	3.56
Crystal size (mm)	$0.20 \times 0.15 \times 0.17$
Radiation type	Mo$K\alpha$ (0.71073 Å)
θ–range for data collection (º)	3.5-32.3
R_{int} (%)	3.13
Reflections collected	18039
Independent reflections	4911
$F_o > 4\sigma(F)$	4389
Refinement method	least-squares matrix: full
No. of refined parameters	300
Final R_{obs} (%) all data	4.14
R_1 (%) $F_o > 4\sigma(F)$	3.47
wR_2 (%) $F_o > 4\sigma(F)$	8.61
Highest peak/deepest hole (e$^-$ Å^{-3})	+0.81 / -0.66
Goodness of fit on F^2	1.191

Table 3. Crystal data and summary of parameters describing data collection and refinement
for braccoite

Table 4.

	Site occupancy	x/a	y/b	z/c	U_{iso}
Na(1)	1 Na$^+$	½	0	½	0.0300(5)
Na(2)	0.521(6) Na$^+$	0.1912(3)	0.5340(2)	0.4432(3)	0.0151(7)
Mn(1)	0.953(5) Mn^{2+} 0.047(5) Mg^{2+}	0.74388(5)	0.97982(5)	0.29542(6)	0.01168(14)
Mn(2)	0.917(5) Mn^{2+} 0.083(5) Mg^{2+}	0.99723(5)	0.21282(5)	0.22004(6)	0.01045(15)
Mn(3)	0.843(5) Mn^{2+} 0.157(5) Mg^{2+}	0.86298(5)	0.88807(5)	0.02950(6)	0.00981(16)
Mn(4)	0.944(5) Mn^{2+} 0.056(5) Mg^{2+}	0.57398(5)	0.66844(4)	0.09774(5)	0.00999(15)
Mn(5)	0.953(5) Mn^{2+} 0.047(5) Mg^{2+}	0.71912(5)	0.55370(5)	0.85346(6)	0.01242(15)
T(1)	1 Si^{4+}	0.87449(9)	0.27556(8)	0.82439(10)	0.00920(15)
T(2)	1 Si^{4+}	0.03102(9)	0.23894(8)	0.60955(9)	0.00861(15)
T(3)	1 Si^{4+}	0.20746(9)	0.54939(8)	0.77372(10)	0.00943(15)
T(4)	1 Si^{4+}	0.47814(9)	0.75745(8)	0.73037(9)	0.00925(15)
T(5)	1 Si^{4+}	0.61959(9)	0.07757(8)	0.89560(9)	0.00829(15)
T(6)	0.465(3) Si^{4+} 0.535(3) As	0.60697(5)	0.71401(4)	0.48355(5)	0.00903(12)
O(1)	1 O	0.7048(2)	0.1654(2)	0.7947(3)	0.0132(4)
O(2)	1 O	0.8853(2)	0.2267(2)	0.6567(3)	0.0145(4)
O(3)	1 O	0.1110(2)	0.4094(2)	0.6204(3)	0.0133(4)
O(4)	1 O	0.3022(2)	0.6692(2)	0.7062(3)	0.0124(4)
O(5)	1 O	0.4987(2)	0.9265(2)	0.7529(3)	0.0128(4)
O(6)	1 O	0.4645(2)	0.7114(2)	0.5465(3)	0.0142(4)
O(7)	1 O	0.8556(3)	0.4331(2)	0.8222(3)	0.0144(4)
O(8)	1 O	0.9645(2)	0.7248(2)	0.0081(3)	0.0118(4)
O(9)	1 O	0.9535(2)	0.1532(2)	0.4220(2)	0.0123(4)
O(10)	1 O	0.8287(2)	0.8130(2)	0.2469(2)	0.0110(4)
O(11)	1 O	0.0805(2)	0.6058(2)	0.8035(3)	0.0143(4)
O(12)	1 O	0.6649(2)	0.4918(2)	0.0594(2)	0.0114(4)
O(13)	1 O	0.3746(2)	0.2765(2)	0.1181(2)	0.0113(4)
O(14)	1 O	0.4961(2)	0.1480(2)	0.9102(3)	0.0127(4)
O(15)	1 O	0.2404(2)	0.9490(2)	0.9367(2)	0.0112(4)
O(16)	1 O	0.6809(3)	0.8807(2)	0.4750(3)	0.0148(4)
O(17)	1 O	0.5172(2)	0.6042(2)	0.2977(3)	0.0137(4)
O(18)	1 O	0.2568(3)	0.3469(2)	0.3699(3)	0.0149(4)
O(19)	1 O	0.0897(2)	0.0502(2)	0.1728(3)	0.0134(4)
H(7)	1 H	0.937(5)	0.493(4)	0.820(5)	0.017***
H(19)**	1 H	0.179(3)	0.050(4)	0.276(3)	0.016***

Notes: *The temperature factor has the form exp(-T) where T = 8 (π^2)U(sin(θ)/λ)^2 for isotropic atoms. **Atom coordinates refined with a soft constraint to O-H of 0.98 Å, ***U_{iso} refined constrained to be 1.2 the isotropic equivalent of the oxygen atom of the hydroxyl group

Table 4. Multiplicities, fractional atom coordinates, and equivalent isotropic displacement parameters (Å^2) for braccoite*

Table 5.

	U_{11}	U_{22}	U_{33}	U_{12}	U_{13}	U_{23}
Na(1)	0.0487(13)	0.0380(12)	0.0215(10)	0.0280(10)	0.0230(10)	0.0175(9)
Na(2)	0.0233(13)	0.0130(12)	0.0087(11)	0.0032(9)	0.0090(10)	0.0023(8)
Mn(1)	0.0098(2)	0.0107(2)	0.0128(2)	0.00149(16)	0.00516(17)	0.00090(16)
Mn(2)	0.0103(2)	0.0107(2)	0.0104(2)	0.00265(16)	0.00545(17)	0.00342(16)
Mn(3)	0.0098(2)	0.0093(2)	0.0112(2)	0.00304(17)	0.00566(18)	0.00310(16)
Mn(4)	0.0093(2)	0.0091(2)	0.0111(2)	0.00244(16)	0.00485(17)	0.00261(15)
Mn(5)	0.0125(2)	0.0113(2)	0.0153(2)	0.00397(17)	0.00813(18)	0.00284(16)
T(1)	0.0087(3)	0.0102(3)	0.0101(3)	0.0031(3)	0.0055(3)	0.0040(3)
T(2)	0.0085(3)	0.0092(3)	0.0079(3)	0.0025(3)	0.0039(3)	0.0027(3)
T(3)	0.0086(3)	0.0088(3)	0.0110(3)	0.0021(3)	0.0050(3)	0.0039(3)
T(4)	0.0097(3)	0.0090(3)	0.0093(3)	0.0025(3)	0.0049(3)	0.0038(3)
T(5)	0.0081(3)	0.0091(3)	0.0086(3)	0.0029(3)	0.0044(3)	0.0038(3)
T(6)	0.0098(2)	0.00979(19)	0.00859(19)	0.00275(14)	0.00542(15)	0.00280(13)
O(1)	0.0107(9)	0.0153(9)	0.0142(9)	0.0024(7)	0.0072(8)	0.0071(8)
O(2)	0.0118(9)	0.0220(10)	0.0113(9)	0.0053(8)	0.0069(8)	0.0043(8)
O(3)	0.0159(10)	0.0102(9)	0.0104(9)	0.0016(7)	0.0049(8)	0.0020(7)
O(4)	0.0112(9)	0.0131(9)	0.0129(9)	0.0020(7)	0.0065(7)	0.0052(7)
O(5)	0.0138(9)	0.0087(8)	0.0121(9)	0.0012(7)	0.0045(8)	0.0036(7)
O(6)	0.0129(9)	0.0199(10)	0.0099(9)	0.0037(8)	0.0064(8)	0.0032(8)
O(7)	0.0134(10)	0.0108(9)	0.0214(11)	0.0042(8)	0.0101(8)	0.0058(8)
O(8)	0.0112(9)	0.0132(9)	0.0112(9)	0.0056(7)	0.0046(7)	0.0034(7)
O(9)	0.0137(9)	0.0134(9)	0.0087(9)	0.0022(7)	0.0056(7)	0.0019(7)
O(10)	0.0107(9)	0.0121(9)	0.0091(9)	0.0040(7)	0.0036(7)	0.0023(7)
O(11)	0.0148(10)	0.0140(9)	0.0200(10)	0.0063(8)	0.0120(8)	0.0069(8)
O(12)	0.0115(9)	0.0114(9)	0.0103(9)	0.0035(7)	0.0044(7)	0.0038(7)
O(13)	0.0128(9)	0.0120(9)	0.0103(9)	0.0051(7)	0.0059(7)	0.0040(7)
O(14)	0.0128(9)	0.0140(9)	0.0142(9)	0.0062(7)	0.0078(8)	0.0047(7)
O(15)	0.0115(9)	0.0110(9)	0.0104(9)	0.0034(7)	0.0048(7)	0.0044(7)
O(16)	0.0175(10)	0.0130(9)	0.0136(10)	0.0031(8)	0.0081(8)	0.0048(8)
O(17)	0.0142(9)	0.0142(9)	0.0105(9)	0.0017(8)	0.0060(8)	0.0003(7)
O(18)	0.0133(9)	0.0159(10)	0.0165(10)	0.0068(8)	0.0066(8)	0.0069(8)
O(19)	0.0125(9)	0.0153(9)	0.0112(9)	0.0049(8)	0.0044(8)	0.0034(7)

Notes: * The temperature factor has the form exp(-T) where $T = 2\pi^2\Sigma_{ij}(h(i)h(j)U(i,j)a*(i)a*(j))$.

Table 5. Anisotropic displacement parameters for braccoite (Å)*

Table 6.

Na(1) - O(5) (×2)	2.444(2)	Mn(2) - O(11)	2.119(2)	Mn(5) - O(7)	2.108(2)	T(3) - O(11)	1.604(2)	T(6) -O(16)	1.646(2)
- O(16) (×2)	2.451(2)	- O(9)	2.136(2)	- O(17)	2.159(2)	- O(12)	1.618(2)	-O(17)	1.667(2)
- O(1) (×2)	2.613(2)	- O(19)	2.161(2)	- O(13)	2.178(2)	- O(4)	1.628(2)	-O(18)	1.670(2)
- O(6) (×2)	2.877(2)	- O(15)	2.189(2)	- O(12)	2.231(2)	- O(3)	1.642(2)	-O(6)	1.719(2)
<Na(1) - O>	2.596	- O(18)	2.222(2)	- O(8)	2.270(2)	<T(3) - O>	1.623	<T(6) - O>	1.675
**$V(\text{Å}^3)$	26.007	- O(8)	2.346(2)	- O(18)	2.374(2)	$V(\text{Å}^3)$	2.188	$V(\text{Å}^3)$	2.403
		<Mn(2) - O>	2.196	<Mn(5) - O>	2.220	σ^2*	7.846	σ^2*	12.945
Na(2) - O(18)	2.285(3)	$V(\text{Å}^3)$	13.711	$V(\text{Å}^3)$	14.066	λ*	1.0019	λ*	1.0032
- O(4)	2.292(3)	σ^2*	67.545	σ^2*	86.772				
- O(7)	2.293(3)	λ*	1.0207	λ*	1.0260	T(4) - O(13)	1.602(2)		
- O(3)	2.355(3)					- O(4)	1.612(2)		
- O(6)	2.484(3)	Mn(3) - O(19)	2.116(2)	T(1) - O(8)	1.613(2)	- O(5)	1.633(2)		
- O(11)	2.513(3)	- O(8)	2.156(2)	- O(1)	1.617(2)	- O(6)	1.643(2)		
- O(2)	2.753(3)	- O(19)	2.163(2)	- O(7)	1.626(2)	<T(4) - O>	1.623	H(7) -O(7)	0.86(4)
- O(3)	2.944(3)	- O(13)	2.191(2)	- O(2)	1.632(2)	$V(\text{Å}^3)$	2.181	H(7) …O(11)	1.62(4)
<Na(2) - O>	2.490	- O(15)	2.199(2)	<T(1) - O>	1.622	σ^2*	14.064	O(7) …O(11)	2.48(1)
$V(\text{Å}^3)$	25.210	- O(10)	2.272(2)	$V(\text{Å}^3)$	2.178	λ*	1.0033	O(7)- H(7)…O(11)	176.37(2)°
		<Mn(3) - O>	2.183	σ^2*	15.761				
Mn(1) - O(9)	2.069(2)	$V(\text{Å}^3)$	13.523	λ*	1.0038	T(5) - O(14)	1.592(2)	H(19) -O(19)	0.95(2)
- O(10)	2.150(2)	σ^2*	55.177			- O(15)	1.607(2)	H(19) …O(16)	1.99(2)
- O(16)	2.177(2)	λ*	1.0174	T(2) - O(9)	1.596(2)	- O(1)	1.634(2)	O(19) …O(16)	2.855(10)
- O(14)	2.190(2)			- O(10)	1.626(2)	- O(5)	1.679(2)	O(19)- H(19)…O(16)	150.34(18)°
- O(15)	2.308(2)	Mn(4) - O(14)	2.107(2)	- O(2)	1.635(2)	<T(5) - O>	1.628		
- O(5)	2.627(2)	- O(12)	2.190(2)	- O(3)	1.647(2)	$V(\text{Å}^3)$	2.183		
<Mn(1) - O>	2.253	- O(17)	2.199(2)	<T(2) - O>	1.626	σ^2*	41.722		
$V(\text{Å}^3)$	14.087	- O(10)	2.220(2)	$V(\text{Å}^3)$	2.200	λ*	1.0098		
σ^2*	170.515	- O(12)	2.246(2)	σ^2*	9.140				
λ*	1.0617	- O(13)	2.287(2)	λ*	1.0021				
		<Mn(4) - O>	2.208						
		$V(\text{Å}^3)$	13.939						
		σ^2*	67.478						
		λ*	1.0204						

Notes: *Mean quadratic elongation (λ) and the angle variance (σ^2) were computed according to Robinson *et al*. (1971); ** V = polyhedral volume

Table 6. Main interatomic distances (Å) and geometrical parameters for braccoite

Table 7.

	T(1)	T(2)	T(3)	T(4)	T(5)	T(6)	M(1)	M(2)	M(3)	M(4)	M(5)	Na(1)	Na(2)	H(7)	H(19)		+ H contrib
O(1)	1.013				0.968							0.115 ×2↓				2.096	
O(2)	0.975	0.965											0.047			1.987	
O(3)		0.937	0.949										0.116 0.030			2.032	
O(4)			0.985	1.026									0.134			2.145	
[IV]O(5)				0.972	0.863		0.120					0.169 ×2↓				2.123	
[IV]O(6)				0.946		1.029						0.063 ×2↓	0.086			2.124	
[IV]O(7)	0.988										0.409		0.133	1.019 0.475		1.531	2.550 2.006
[IV]O(8)	1.024							0.223	0.353		0.271					1.871	
O(9)		1.073					0.457	0.376								1.906	
[IV]O(10)		0.988					0.369		0.264	0.306						1.928	
[IV]O(11)			1.050					0.393					0.081	0.255 0.475		1.524	1.779 1.999
O(12)			1.010							0.331 0.287	0.298					1.927	
[IV]O(13)				1.056					0.323	0.260	0.341					1.980	
O(14)					1.084		0.332				0.410					1.826	
[IV]O(15)					1.041		0.248	0.328	0.317							1.934	
[IV]O(16)						1.240	0.344					0.166 ×2↓			0.162	1.749	1.911
O(17)						1.173			0.323	0.358						1.855	
[IV]O(18)						1.167		0.302		0.211			0.136			1.815	
O(19)							0.353	0.392 0.347							0.824	1.091	1.915
	4.000	3.963	3.994	3.999	3.956	4.609	1.870	1.975	1.996	1.917	1.888	1.026	0.763 0.950	1.274	0.986		37.38
F.C.*	4.000	4.000	4.000	4.000	4.000	4.630	2.000	2.070	2.240	2.030	2.000	1.000	0.560	1.000	1.000	37.96	

Note: anion sites coordination reported only for coordination other than 3. * F.C: = formal charge at site on the basis of chemical formula

Table 7. Bond valence calculations for braccoite (Brown, 1981)

Table 8.

Site	Refined site-scattering (apfu) (epfu)	Assigned site-population	Calculated site-scattering (epfu)	$\langle X\text{-}\varphi\rangle_{calc.}$* (Å)	$\langle X\text{-}\varphi\rangle_{obs.}$ (Å)	Ideal composition (apfu)
		Cations				
Mn(1)	24.39(7)	$0.98\ Mn^{2+} + 0.01\ Mg + 0.01\ Ca$	24.82	2.191	2.253	Mn^{2+}
Mn(2)	23.93(7)	$0.87\ Mn^{2+} + 0.07\ Mn^{3+} + 0.06\ Mg$	24.22	2.170	2.196	Mn^{2+}
Mn(3)	22.96(7)	$0.56\ Mn^{2+} + 0.32\ Mn^{3+} + 0.10\ Mg + 0.01\ V^{3+} + 0.01\ Al^{3+} +$	23.53	2.130	2.183	Mn^{2+}
Mn(4)	24.28(7)	$0.96\ Mn^{2+} + 0.03\ Mn^{3+} + 0.01\ Mg$	24.87	2.183	2.208	Mn^{2+}
Mn(5)	24.39(7)	$0.99\ Mn^{2+} + 0.01\ Mg$	24.87	2.189	2.220	Mn^{2+}
T(6)	24.17(6)	$0.48\ As + 0.37\ Si + 0.15\ V^{5+}$	24.47	1.671	1.675	As
Na(1)	11	1.00 Na	11.00	2.560	2.596	Na**
Na(2)	5.72(6)	$0.56\ Na + 0.44\ \square$	6.16	2.560	2.490	Na,$\square$
		Anions				
[IV]O(19)		0.98 OH + 0.02 F				OH

X = cation, φ = O, OH, F;
* calculated by summing constituent ionic radii; values from Shannon (1976);
** site in special position, half multiplicity;

Table 8. Refined site-scattering and assigned site-populations for braccoite

Table 9.

	Braccoite	Saneroite	Scheuchzerite	Steedeite
Reference	(1)	(2, 3)	(4)	(5)
Formula	NaMn$^{2+}_5$[Si$_5$AsO$_{17}$(OH)](OH)	NaMn$^{2+}_5$[Si$_5$VO$_{17}$(OH)](OH)	NaMn$^{2+}_9$[Si$_9$O$_{25}$(OH)(VO$_3$)](OH)	NaMn$_2$[Si$_3$BO$_9$](OH)$_2$
Crystal system	Triclinic	Triclinic	Triclinic	Triclinic
Space group	$P\bar{1}$	$P\bar{1}$	$P\bar{1}$	$P\bar{1}$
a (Å)	9.7354(4)	9.741(5)	9.831(5)	6.837(1)
b	9.9572(3)	9.974(7)	10.107(5)	7.575(2)
c	9.0657(3)	9.108(5)	13.855(7)	8.841(2)
α (°)	92.691(2)	92.70(4)	86.222(10)	99.91(3)
β	117.057(4)	117.11(4)	73.383(9)	102.19(3)
γ	105.323(3)	105.30(4)	71.987(9)	102.78(3)
V (Å^3)	740.37(4)	744.16	1254.2(10)	424.81(1)
Z	2	2	2	2
Axial ratios (a:b:c)	0.978:1:0.910	0.977:1:0.913	0.973:1:1.371	0.9026:1:1.1671
D_{meas} (g cm^{-3})	n.d.	3.47	3.50(2)	n.d.
D_{calc} (g cm^{-3})	3.56	3.51	3.47	3.104
Strongest lines in the powder pattern: d_{obs} (Å)(I)	3.774(30), 3.514(30), 3.042(60), 3.005(60), 2.973(80), 2.821(100), 2.696(90), 2.620(30), 2.676(50), 1.673(30)	3.06(s), 2.83(s), 2.70(s), 3.01(m), 2.98(m), 2.62(m), 2.20(m)	2.71(100), 3.09(80), 7.91(70),8.68(50), 2.92(40), 3.22(40), 3.94(30), 4.83(30)	8.454 (100), 7.234(39), 3.331(83), 3.081(38), 2.859(52), 2.823(80)
Optical character	biaxial (+)	biaxial (−)	biaxial (+)	biaxial
Colour	brown-red	bright orange	yellow-orange	pale pink to colourless
Pleochroism	X = brownish yellow, Y = dark yellow , Z = yellow	X = deep orange; Y = lemon-yellow; Z = yellow-orange	X = brown yellow; Y = pale yellow	Not observed
Hardness (Mohs)	n.d.	n.d.	2-3	n.d.
Streak	pale-yellow	white	yellow-orange	white
Luster	vitreous to resinous	resinous to greasy	vitreous	vitreous
Habit and forms	subhedral	tabular-prismatic crystals	acicular and prismatic crystals	acicular crystals
Association	aegirine, hematite, tiragalloite, quartz, unidentified Mn oxides, and Mn silicates	quartz, baryte, caryopilite, ganophyllite, medaite, palenzonaite, pyrobelonite, fianelite, parsettensite, rhodochrosite, kutnahorite, aegirine	saneroite, tiragalloite	aegirine, analcime, catapleiite, eudialyte, microcline nepheline, natrolite, pyrrhotite, sérandite, sodalite, thermonatrite

Refs: (1) this work; (2) Lucchetti *et al.* (1981); (3) Nagashima and Armbruster (2010a); (4) Brugger *et al.* (2006); (5) Haring and McDonald (2014).

Table 8. Comparison of minerals related to braccoite. References are given in brackets

Table 9.

	Saneroite (Molinello mine, Italy)[1]				Saneroite (Fianel, Switzerland)[1]		Braccoite (Valletta mine, Italy)[2]	
	specimen 1		specimen 2					
	Wt%	SD	Wt%	SD	Wt%	SD	Wt%	SD
SiO_2	39.99	1.06	39.06	0.65	41.03	0.98	39.73	0.59
Al_2O_3	0.02	0	0.01	0.02	0.01	0.02	0.04	0.04
MnO	42.2	1.38	40.33	1.06	41.53	1.12	39.00	0.41
Mn_2O_3	-	-	-	-	-	-	3.07	0.53
MgO	0.01	0.02	0.00	0.00	0.03	0.04	0.96	0.05
CaO	0.13	0.05	0.11	0.04	0.33	0.12	0.05	0.01
Na_2O	4.34	0.28	4.36	0.27	4.52	0.25	4.06	0.2
K_2O	0	0.01	0.01	0.01	0.01	0.01	-	-
CuO	0.1	0.14	0.2	0.24	0.14	0.2	0.02	0.01
NiO	0.03	0.04	0.03	0.03	0.02	0.03	-	-
V_2O_5	7.15	1.8	7.78	0.7	6.05	1.23	1.43	0.11
As_2O_5	1.22	1.27	1.92	1.65	1.31	1.85	6.87	0.61
SO_3	-	-	-	-	-	-	0.01	0.01
F	-	-	-	-	-	-	0.04	0
Total	95.19		93.81		94.98		95.28	

Refs: (1) Nagashima and Armbruster, 2010a; (2) this work

Table 9. Comparison of chemical data between saneroite from Molinello mine (Italy) and Fianel (Switzerland) and braccoite from Valleta (this work).

FIGURE CAPTIONS

Figure 1. a) Picture of the rocks containing braccoite; b) Picture of rare red crystalline masses with brown hue of braccoite holotype intergrown with orange tiragalloite forming a thin layer on hematite and quartz (FoV: 5 mm). Photo of R. Bracco.

Figure 2. BSE image of a section of a quartz (qtz) vein showing braccoite (brac) and tiragalloite (tirag) used during the WDS analyses. Small spot within quartz is baryte (bary)

Figure 3. Raman spectra of braccoite in the 200-4000 cm^{-1} region and between 200 and 1200 cm^{-1}.

Figure 4. Raman spectra of tiragalloite in the 150-4000 cm^{-1} region and between 150 and 1200 cm^{-1}.

Figure 5. Detail of the braccoite structure showing the bands of Mn octahedra and the silicate chains. Blue: Si tetrahedra; green: As-Si tetrahedron; yellow: Mn octahedra; light blue: Na.; white: H. Violet double arrow shows the short $Na(2)…H(7)$ distance. Approx. vector of projection is [5̄15]. Design obtained with Vesta 3 (Momma and Izumi, 2011).
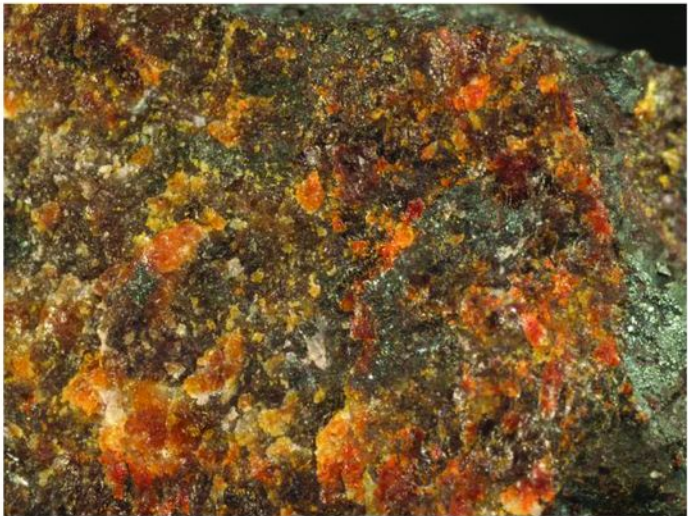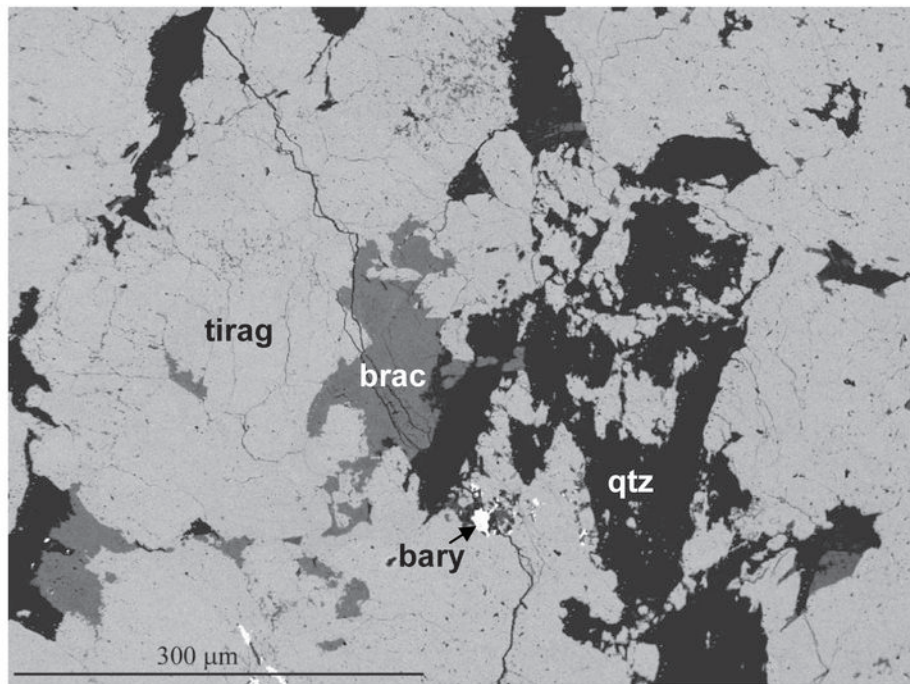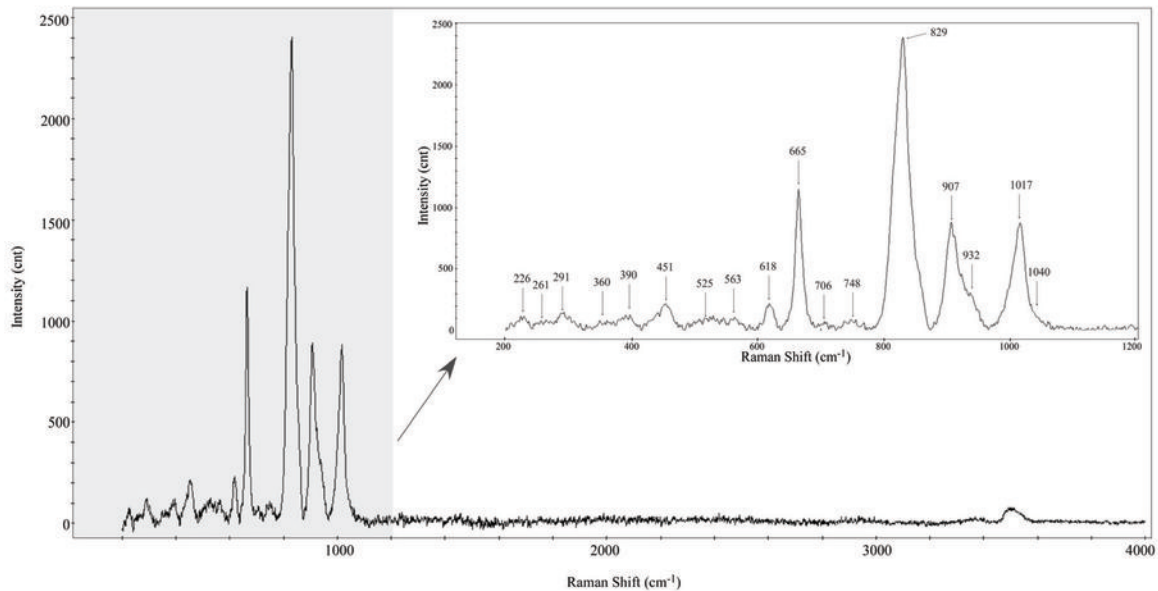
Figure 1a.
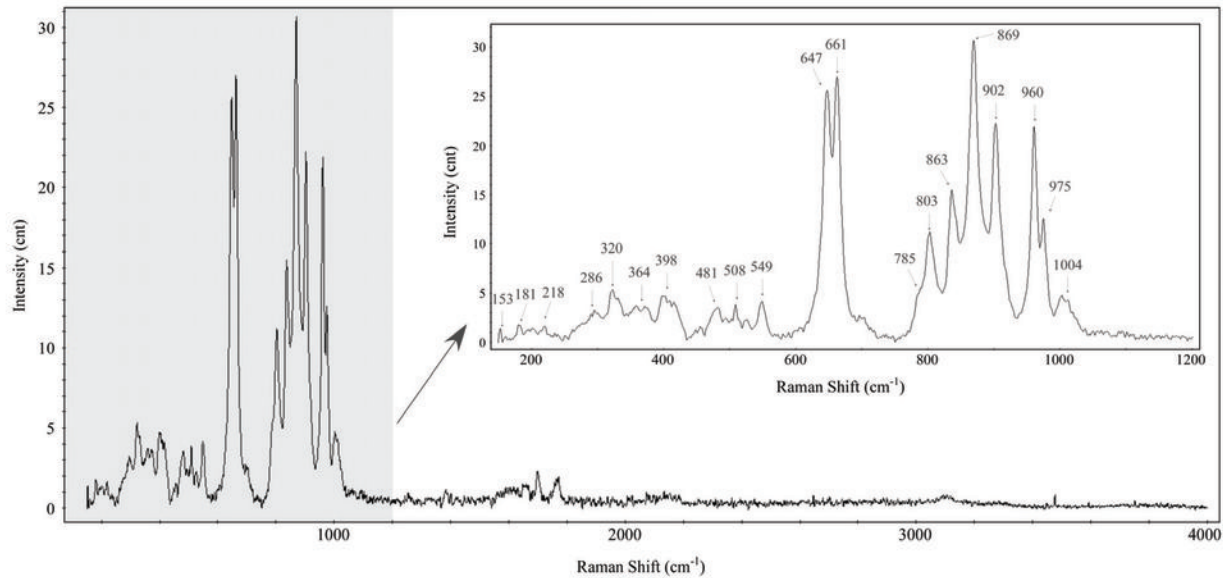
Figure 1b.

Figure 2.

Figure 3.

Figure 4.

Figure 5.